

Supporting Information

Tuning the Composition of Heavy Metal-free Quaternary Quantum Dots for Improved Photoelectrochemical Performance

Cheng Liu¹, Xin Tong^{1,2*}, Ali Imran Channa¹, Xin Li¹, Zhihang Long¹, Huijie Feng¹,
Yimin You¹, Rui Wang¹, Feng Lin¹, Chang Fu Dee⁵, Alberto Vomiero^{3,4*}, Zhiming M.
Wang^{1,5*}

1. Institute of Fundamental and Frontier Sciences, University of Electronic Science and Technology of China, Chengdu 610054, P. R. China.

2. Yangtze Delta Region Institute (Huzhou), University of Electronic Science and Technology of China, Huzhou 313001, P. R. China.

3. Division of Materials Science, Department of Engineering Sciences and Mathematics, Luleå University of Technology, SE-97187 Luleå, Sweden.

4. Department of Molecular Sciences and Nanosystems, Ca' Foscari University of Venice, Via Torino 155, 30170 Venezia Mestre, Italy.

5. Institute of Microengineering and Nanoelectronics (IMEN), Universiti Kebangsaan Malaysia, 43600, Bangi, Selangor, Malaysia.

Corresponding authors: xin.tong@uestc.edu.cn; alberto.vomiero@ltu.se;
zhmwang@uestc.edu.cn

Experimental Section

Material

Copper (I) iodide (CuI, 98%), indium acetate (In(Ac)₃, 99.99%), zinc acetate dihydrate (Zn(Ac)₂·2H₂O, 98%), 1-dodecanethiol (DDT, 98%), oleic acid (OA, 90%), sulfur

powder (S, 99.99%), Oleylamine (OLA, 70%), 1-octadecene (ODE, 90%), anhydrous sodium sulfite (Na_2SO_3 , 98%), Sodium sulfide nonahydrate ($\text{Na}_2\text{S}\cdot 9\text{H}_2\text{O}$, 99%), Hexadecyl trimethyl ammonium Bromide (CTAB, 90%), isopropanol (IPA), ethanol, toluene and methanol were purchased from Sigma-Aldrich. Zirconium dioxide (ZrO_2) was purchased from Aladdin. Titania paste (18 NR-AO) was obtained from Dyesol (Queanbeyan, Australia). Ti-Nanoxide BL/SC was bought from Solaronix. All chemicals were used without further purification.

CuZnInS₃ quantum dots (CZIS QDs) synthesis

CZIS QDs were synthesized by the procedures reported by Ruwini et al., [1]. Typically, the valence states of Cu, Zn, In and S were assumed to be +1, +2, +3 and -2 respectively, to achieve stoichiometric ratio of Cu: Zn: In: S to be 1:1:1:3. CuI (0.2 mmol, ~38.1 mg), $\text{Zn}(\text{Ac})_2\cdot 2\text{H}_2\text{O}$ (0.2 mmol, ~43.9 mg), $\text{In}(\text{Ac})_3$ (0.2 mmol, ~58.4 mg), OA (0.3 mL), DDT (0.5 mL) and ODE (8 mL) were first loaded into a three neck flask connected with nitrogen cylinder and vacuum pump through Schlenk line system. Subsequently, the mixture was degassed at 110 °C under a stable nitrogen flow for 10 min. The pump was then removed and the temperature was raised to 170 °C rapidly under N_2 flow. After the solution got clear and transparent, the reaction system was naturally cooled down to 150 °C. OLA-S solution (0.15 M) (~4 mL) prepared by dissolving the sulfur powder (0.6 mmol, ~19.2 mg) in 4 mL OLA was then swiftly injected into the flask. The temperature was maintained at 150 °C for 10 min for the nucleation and growth of QDs and the reaction was finally quenched with cold water. As-synthesized QDs (1 mL) were precipitated and purified by mixture of toluene (1 mL) and ethanol (4 mL) and

centrifuged at 8000 r.p.m for 3 min. This purification process was repeated at least twice and finally the QDs were re-dispersed in toluene (7 mL) and stored at - 10 °C for further process. CZIS QDs with different Zn composition, i.e. Cu: Zn ratio of 1:0.5, 1:1 and 2:1 were synthesized using the same procedures and reaction conditions mentioned above and marked as CZIS (0.5Zn,1Zn and 2Zn) QDs, respectively. The product yield which was estimated to be ~89%, which was roughly calculated by weighing the obtained quantum dot powder products with repeated purification (removal of the surface ligand effect) as relative to the theoretical weights of initial precursors.

Preparation of TiO₂ and ZrO₂ mesoporous films

The FTO substrates were soaked and cleaned by toluene (~50 mL), ethanol (~50 mL) and deionized water (~50 mL) in ultrasonic machine for 30 min, respectively. Subsequently, FTO was dried by N₂ flow, followed by spin-coating a TiO₂ blocking layer employing Ti-Nanoxide BL/SC solution (50 µL) at 5000 r.p.m for 30 s and then heated at 500 °C for 30 min. Ultimately, a thick TiO₂ film was deposited on FTO substrates by tape-casting using commercial Titania paste (18 NR-AO) followed by sintering at 500 °C for 30 min.

ZrO₂ film was prepared by dissolving 1 g of ZrO₂ powder in 5 mL of IPA in a beaker with subsequent 12-hour magnetic stirring. The solvent was removed by continuous magnetic stirring and pumping until the volume of the mixture reduced to half of starting volume. A single layer ZrO₂ film was deposited on FTO glass by tape casting and then annealed in a furnace at 450 °C for 30 min.

Fabrication of QDs-sensitized photoanode

Chemical bath deposition (CBD) was employed for the sensitization of QDs into mesoporous TiO₂ films. Generally, the TiO₂/FTO/glass (T-FTO) as photoanodes were immersed into the purified QDs solution (~6 mL) in toluene, which is subsequently sealed and kept in a dark place at room temperature for 24 h. Toluene was then applied to gently rinse the surface of QDs-sensitized T-FTO. Successive ionic layer adsorption and reaction (SILAR) approach was employed to deposit ZnS layer on the QDs-sensitized T-FTO electrode. Prior to ZnS deposition, the QDs-based photoelectrodes were immersed in 0.1 M CTAB-methanol solution (~20 mL) for 60 s and rinsed with methanol, this procedure was repeated twice for ligand exchange. For ZnS deposition, the electrode was immersed into 0.1 M Zn(Ac)₂-methanol solution (~20 mL) and 0.1 M Na₂S-methanol/deionized water (volume ratio 1:1) solution (~20 mL) for 60 s. After each immersion, the corresponding solvents (~20 mL) were used to wash off the excessive precursor on the electrode surface. In this work, different SILAR cycles were conducted for the deposition of 2, 4, 6 and 8 ZnS monolayers on the QDs-based photoanodes, which were then dried under N₂ flow. Finally, the photoanode surface was covered by epoxy resin excluding the active area of ~0.1 cm².

Characterization

UV-Vis absorption spectra were taken by Varian Cary 5000 UV-Vis-NIR spectrophotometer (Varian). Photoluminescence (PL) spectra and PL lifetime of QDs were measured via FLS 920 fluorescence spectrometer with 420 nm laser excitation. Photoluminescence quantum yield (PLQY) was obtained by Absolute PL Quantum Yield Measurement System (C9920-02G). Transmission electron microscopy (TEM)

images and selected area electron diffraction (SAED) pattern was carried out by FEI TECNAI G2 F20 HRTEM. Scanning electron microscope (SEM) and energy dispersive X-ray spectroscopy (EDS) mapping were obtained by ZEISS Gemini SEM 300 system equipped with an EDS detector. X-ray diffraction (XRD) patterns were recorded using a Bruker D8 ADVANCE A25X with Cu K α radiation. X-ray photoelectron spectroscopy (XPS) were performed by a Thermo Fisher Scientific Escalab 250Xi high vacuum system, and the data was analyzed by CasaXPS software.

The PEC performance was evaluated by using electrochemical workstation (PARSTAT 3000A-DX with 20 mV/s sweep rate) with class AAA solar simulator (SAN-EI, XES-50S1) under 1 sun illumination (AM 1.5G, 100 mW/cm², calibrated through a Si reference cell before each measurement) as well as a standard three-electrode system consisting of QDs-sensitized photoanode as working electrode, Ag/AgCl as reference electrode (saturated in 3M KCl) and Pt foil as counter electrode. The default electrolyte solution A (solA) (100 mL) (pH~12.5) is composed of 0.25 M Na₂S and 0.35 M Na₂SO₃ and the neutral electrolyte solution B (solB) (100 mL) (pH~7) is composed of 0.2 M Na₂SO₄. The Electrochemical impedance spectroscopy (EIS) plots and Mott-Schottky curves were collected via the above-mentioned three-electrode system under parameters of 0.1 Hz to 10 kHz with 10 mV amplitude at 0 V bias and a fixed frequency of 1000 Hz with 10 mV amplitude of open circuit potentials, respectively. The hydrogen yield of QDs-PEC cell was measured by gas chromatography system (Shimadzu GC-2014) under applied bias of 0.6 V (vs. RHE).

Calculation of Incident photon-to-electron conversion efficiencies (IPCEs)[2]

$$IPCE = \frac{1240 \times J_{sc}(\mu A/cm^2)}{\lambda(nm) \times P(\mu W/cm^2)}$$

Where $J_{sc}(\mu A/cm^2) = I_{DSC}(\mu A)/S_{DSC}(cm^2)$ represents the saturated photocurrent of $I_{DSC}(\mu A)$ per unit active area of $S_{DSC}(cm^2)$ under monochromatic incident light provided by solar simulator equipped with band-pass filters. $\lambda(nm)$ and $P(\mu W/cm^2)$ is the wavelength and optical power density of monochromatic light, respectively.

Calculation of theoretical yield of hydrogen

$$H_2(mole) = \frac{Q}{2F} = \frac{I \times t}{2F} = \int_0^t \frac{I dt}{F}$$

Where Q, F and I are the quantity of the charge passed through the circuit in time t , Faraday's constant (96484.34 C/mol) and obtained photocurrent from the photoanode, respectively [3]. In our case, the amount of the charge Q was calculated by integrating the current (I) over time (t) in **Figure S11**.

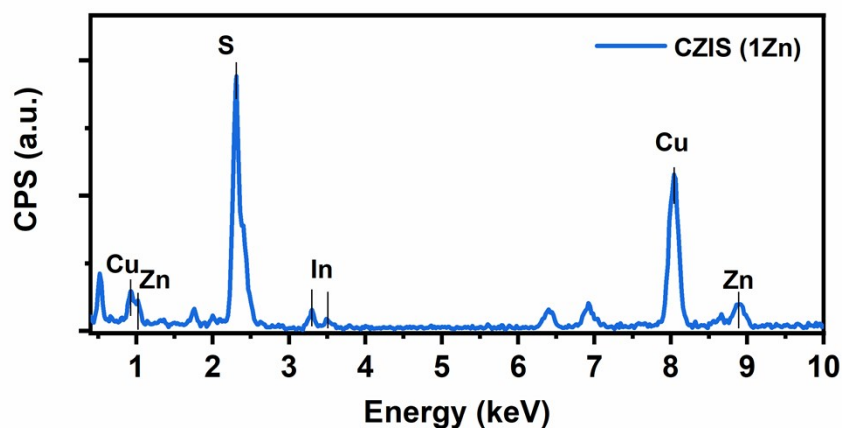


Figure S1. EDS spectrum of CZIS (1Zn) QDs showing the existence of Cu, Zn, In and S elements.

Table S1. Comparison of crystal structure data of chalcopyrite CuInS₂ and CZIS (1Zn) QDs.

Crystal plane	CuInS ₂		CZIS (1Zn)	
	d-value	I/I ₀	d-value	I/I ₀
(112)	0.319	999	0.316	999
(220)	0.195	357	0.191	497
(312)	0.166	232	0.164	294
Reference	JCPDS No. 75-0106		Our SAED data	

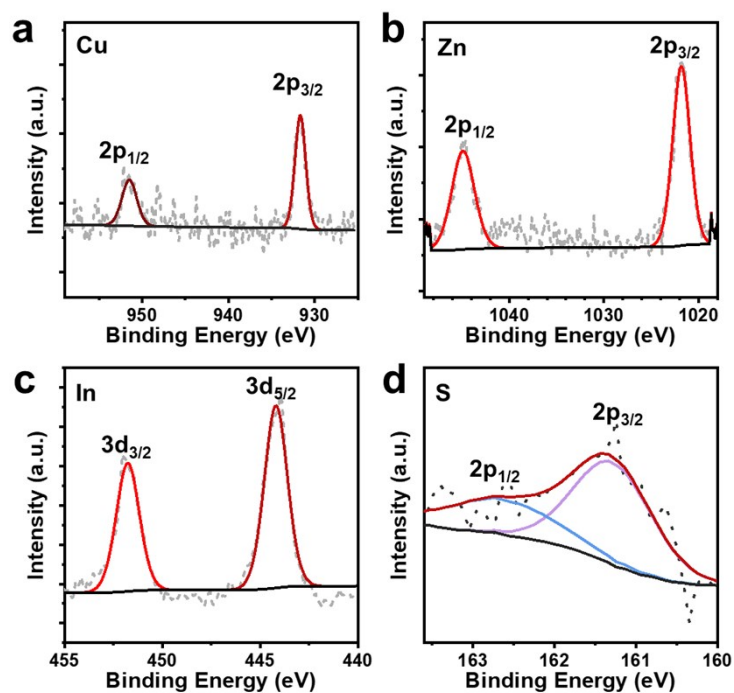


Figure S2. HRXPS spectra of (a) Cu, (b) Zn, (c) In and (d) S in CZIS (0.5Zn) QDs.

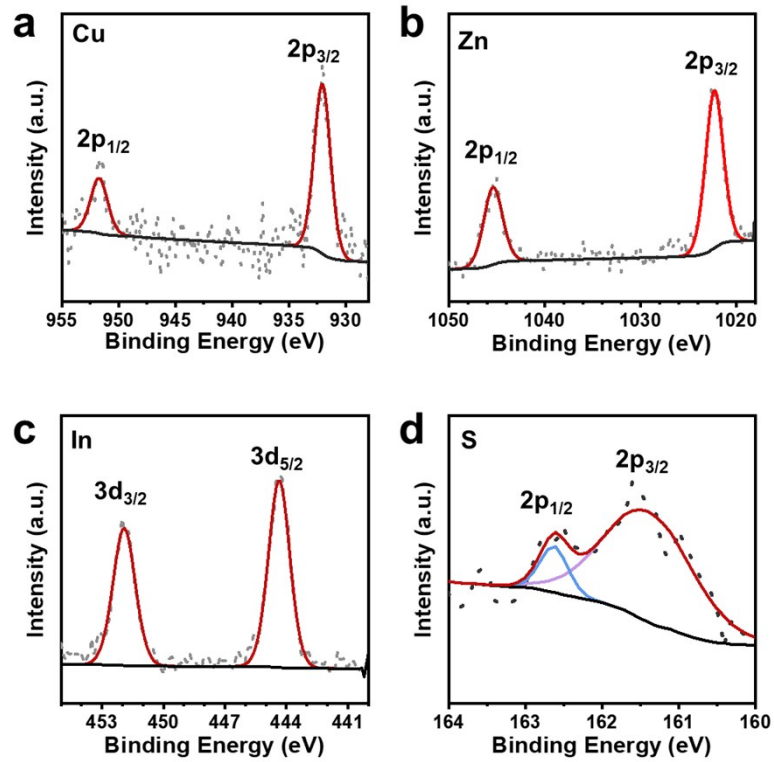


Figure S3. HRXPS spectra of (a) Cu, (b) Zn, (c) In and (d) S in CZIS (1Zn) QDs.

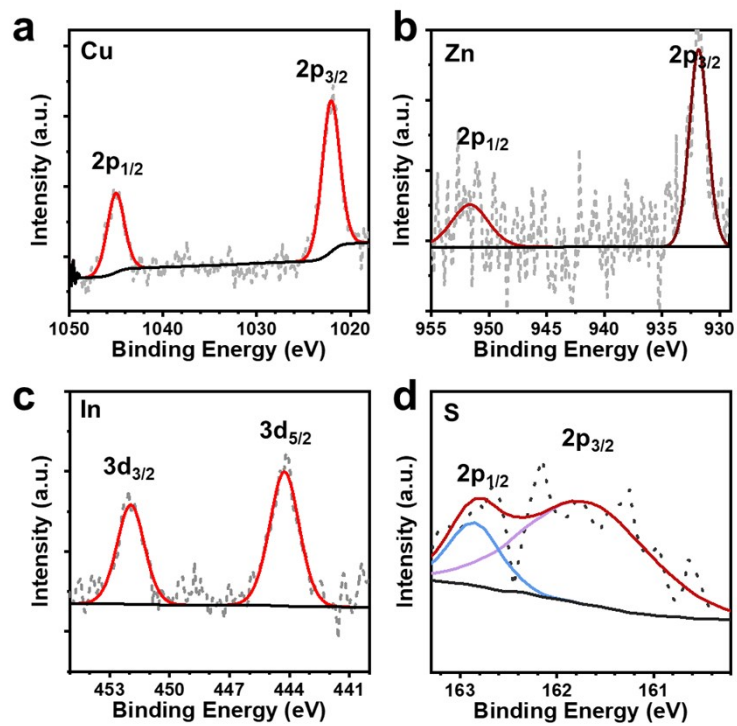


Figure S4. HRXPS spectra of (a) Cu, (b) Zn, (c) In and (d) S in CZIS (2Zn) QDs.

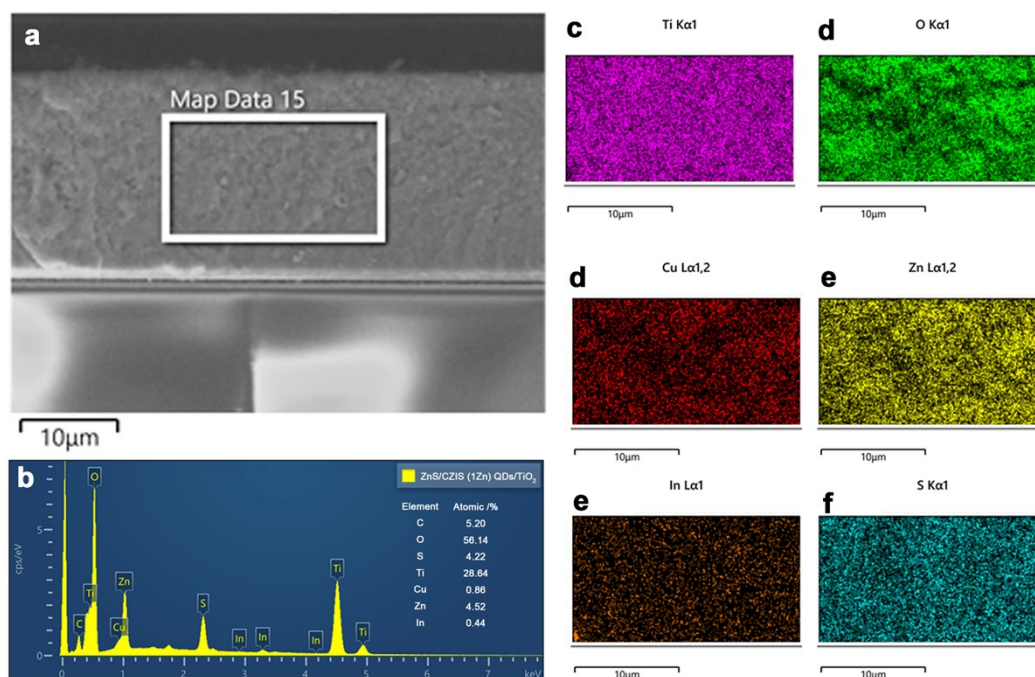


Figure S5. (a) Cross-sectional SEM images of CZIS (1Zn) QDs-based photoelectrode with a white box showing the EDS spectrum and mapping area. (b) EDS spectrum of CZIS (1Zn) QDs-sensitized mesoporous TiO₂ film. (c)-(f) EDS mapping scan of CZIS (1Zn) QDs-sensitized TiO₂ photoelectrode, demonstrating the existence of Ti, O, Cu, Zn, In and S elements in the TiO₂ film.

Table S2. XPS analysis of CZIS (0.5Zn), CZIS (1Zn) and CZIS (2Zn) QDs.

XPS Peak	Cu		Zn		In		S		
	Cu 2p _{1/2}	Cu 2p _{3/2}	Zn 2p _{1/2}	Zn 2p _{3/2}	In 3d _{3/2}	In 3d _{5/2}	S 2p _{1/2}	S 2p _{3/2}	
CZIS (2Zn)	B. E (eV)	951.63	931.81	1045.02	1022.06	451.93	444.23	162.83	161.69
	Area	487.7	1142.7	3414	6707.5	865.4	1261	76.9	305
CZIS (1Zn)	B. E (eV)	951.71	932.05	1045.37	1022.27	451.92	444.35	162.63	161.40
	Area	660.7	1951.3	4161	8007	1923.7	2510.9	67.5	508.6
CZIS (0.5Zn)	B. E (eV)	951.49	931.67	1044.88	1021.81	451.77	444.19	162.63	161.29
	Area	1011.2	1805.5	4611.2	6415.1	1976.3	2799.4	141.9	286.8
R.S.F(from XPS)		5976.24		4512.42		9567.57		602.59	
Semi quantitative element ratio	(2Zn)**	1.00		8.22		0.81		2.32	
	(1Zn)**	1.00		6.17		1.06		2.19	
	(0.5Zn)**	1.00		5.18		1.06		1.51	

* B. E stands for binding energy.

** The signal of S 2p is not clear in CZIS QDs, so the rate of S in CZIS is not precise, and just for reference only.

Table S3. Detailed parameters of PL peaks fitting including position, FWHM and intensity of CZIS (0.5Zn), CZIS (1Zn) and CZIS (2Zn) QDs.

Samples	PL	Peak1			Peak2			Area ratio of Peak1 and Peak2
	Position /nm	Position /nm	FWHM /nm	Area /a.u.	Position /nm	FWHM /nm	Area /a.u.	
CZIS (0.5Zn)	650	638	82	47.9	679	130	75.5	0.63
CZIS (1Zn)	617	610	89	83.3	668	130	44.6	1.87
CZIS (2Zn)	587	578	76	57.1	630	113	58	0.98

Table S4. The parameters for tri-exponential PL lifetime decay fitting of CZIS (1Zn) QDs with different excitation wavelength, the error bar is obtained by conducting three times fitting.

QDs	Excitation wavelength	A ₁ /%	τ ₁ /ns	A ₂ /%	τ ₂ /ns	A ₃ /%	τ ₃ /ns	τ _{av} /ns
CZIS (1Zn)	420 nm	1	1.5	13	9.8	86	67.4	66±2
	510 nm	1	1.6	14	10.6	85	69.6	68±2

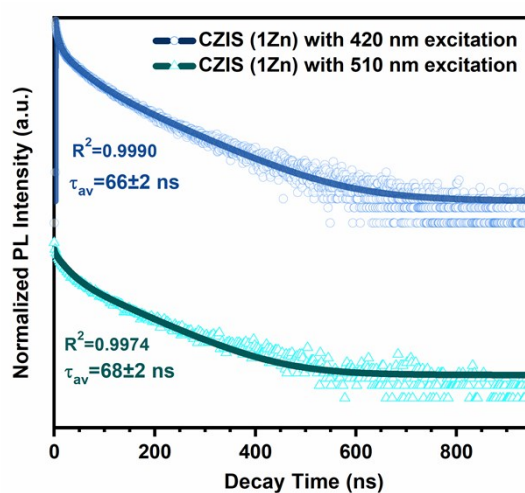


Figure S6. Decay of PL intensity versus time of CZIS (1Zn) QDs with different excitation wavelength, the error bar is obtained by conducting three times fitting.

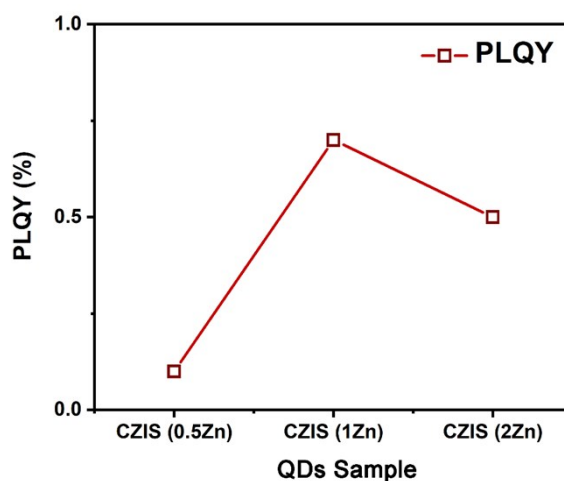


Figure S7. The PLQY plots of CZIS (0.5Zn), CZIS (1Zn) and CZIS (2Zn) QDs.

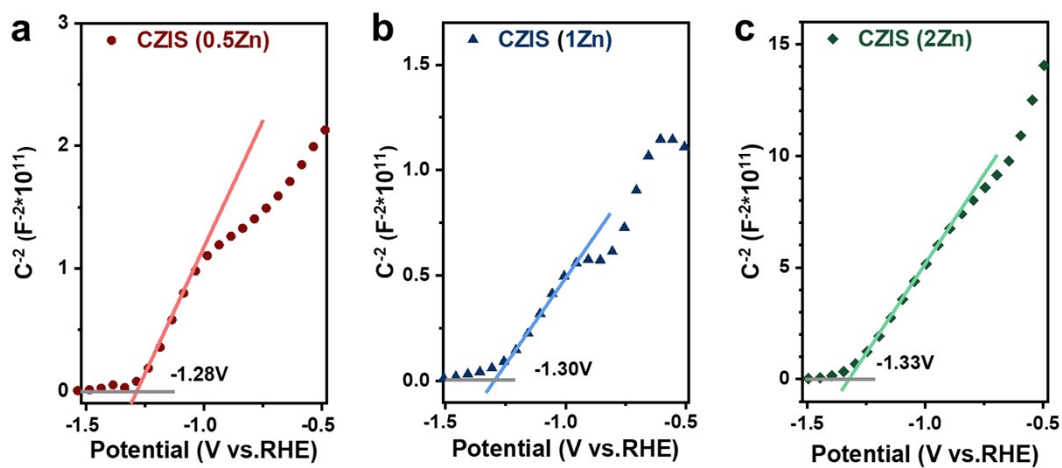


Figure S8. Mott-Schottky plots of (a) CZIS (0.5Zn), (b) CZIS (1Zn) and (c) CZIS (2Zn) QDs-sensitized photoanodes without any ZnS layer under a fixed frequency of 1000 Hz with 10 mV amplitude of open circuit potentials, respectively.

Table S5. The slope and relevant reciprocal in Mott-Schottky plots of QDs-sensitized photoanodes.

Samples	Slope	$[d(1/C^2)/dV]^{-1}$
CZIS (0.5Zn)	4.06×10^{11}	2.46×10^{-12}
CZIS (1Zn)	1.63×10^{11}	6.13×10^{-12}
CZIS (2Zn)	1.55×10^{12}	6.45×10^{-13}

Table S6. The parameters for tri-exponential PL lifetime decay fitting of CZIS QDs/TiO₂, CZIS QDs/ZrO₂ electrodes and calculated charge transfer rate constants using the longest lifetime (τ_3).

QDs	Substrates	A ₁ /%	τ_1 /ns	A ₂ /%	τ_2 /ns	A ₃ /%	τ_3 /ns	τ_{av} /ns	$k_{et_ \tau_3}/10^8s^{-1}$
CZIS (0.5Zn)	TiO ₂	85	0.19	10	1.2	5	5.4	3.0	0.18
	ZrO ₂	2	0.22	52	1.3	46	6.0	5.1	
CZIS (1Zn)	TiO ₂	68	0.18	22	1.3	10	6.8	4.6	1.01
	ZrO ₂	6	0.45	48	3.7	46	21.7	19.0	
CZIS (2Zn)	TiO ₂	23	0.26	54	1.5	23	8.0	5.9	0.94
	ZrO ₂	79	0.19	11	5.8	10	32.5	27.1	

Table S7. The parameters for the equivalent circuit model fitting of QDs-sensitized photoelectrodes for EIS analysis.

Sample	R ₀ /Ω	CPE ₁		R ₁ /Ω	chi squared
		Q	n		
CZIS (0.5Zn)	19.58	1.03E-05	0.8293	1266	0.10%
CZIS (1Zn)	19.01	1.29E-05	0.8493	699.8	0.17%
CZIS (2Zn)	20.13	1.47E-05	0.7932	1605	0.07%

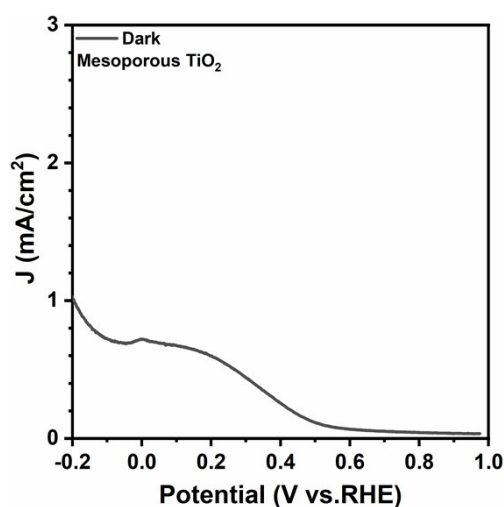


Figure S9. Electrochemistry measurement of bare mesoporous TiO₂/FTO working electrode.

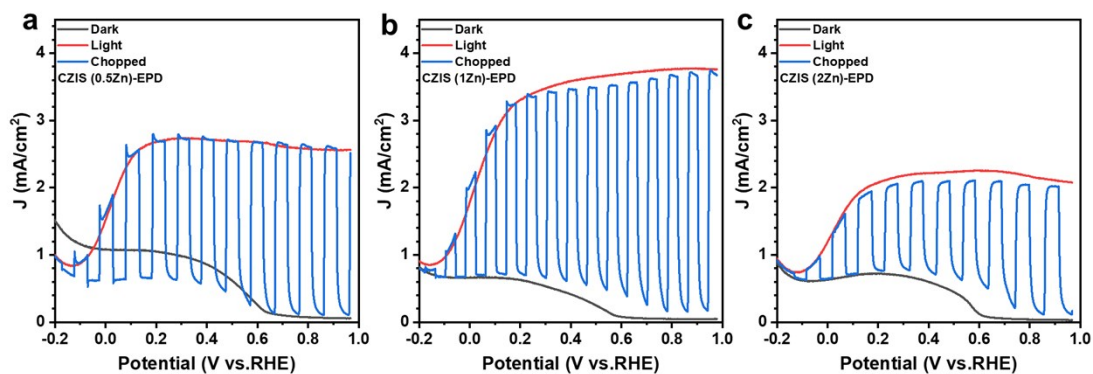


Figure S10. PEC performance of (a) CZIS (0.5Zn), (b) CZIS (1Zn) and (c) CZIS (2Zn) QDs-sensitized photoanodes fabricated by EPD method.

Table S8. Comparison of PEC performance of optimized CZIS (1Zn) QDs-based devices with other similar QDs based PEC systems.

Type of QDs	Structure	Substrate	Photocurrent /mA/cm ²	Stability (2h)/%	Faradaic Efficiency/%	Reference
6ZnS/CZIS (1Zn)	Core	TiO ₂	4.4	71	91	Our work
CuInS ₂	Core	TiO ₂ NWAs	~2.3	-	-	[4]
CuInS ₂	Core	TiO ₂	~1.92	-	-	[5]
CuGaS ₂	Core	TiO ₂	~0.8	50	-	[3]
CZTS	Core	TiO ₂ NT	~0.04	-	-	[6]
Zn-CISe/CIS	Core/Shell	TiO ₂	~3.2	69	-	[10]
CISeS/ZnS	Core/Shell	TiO ₂	5.3	72	-	[7]
MnCIS/ZnS	Core/Shell	TiO ₂	5.7	73	74	[8]

Table S9. PEC performance of CZIS (0.5Zn), CZIS (1Zn) and CZIS (2Zn) QDs-based photoelectrodes fabricated by EPD and CBD method.

	CZIS (0.5Zn)	CZIS (1Zn)	CZIS (2Zn)
CBD method	2.8 mA/cm ²	3.7 mA/cm ²	2.1 mA/cm ²
EPD method	2.5 mA/cm ²	3.7 mA/cm ²	2.0 mA/cm ²

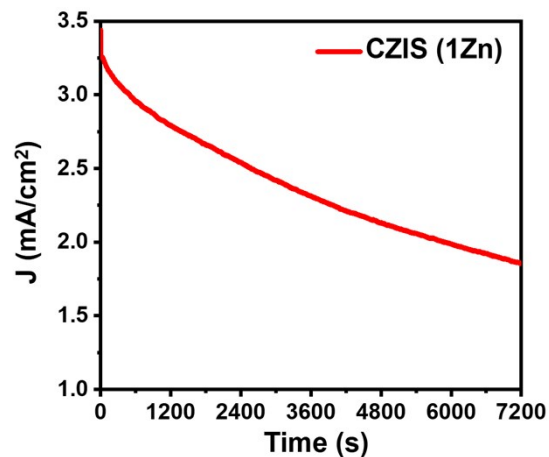


Figure S11. *J-t* curve of CZIS (1Zn) QDs -sensitized photoanode under 1 sun illumination (AM 1.5G, 100 mW/cm²) for 2 hours (7200 seconds) under applied bias of 0.6 V (vs RHE).

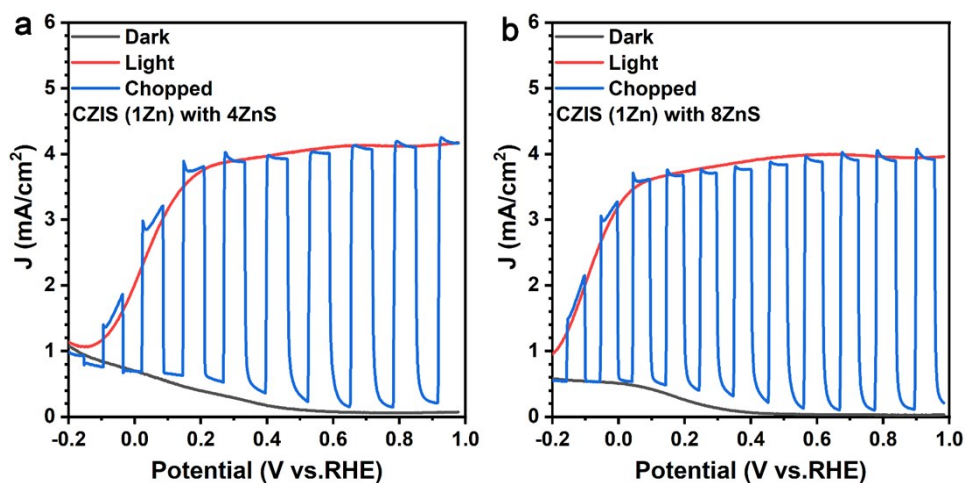
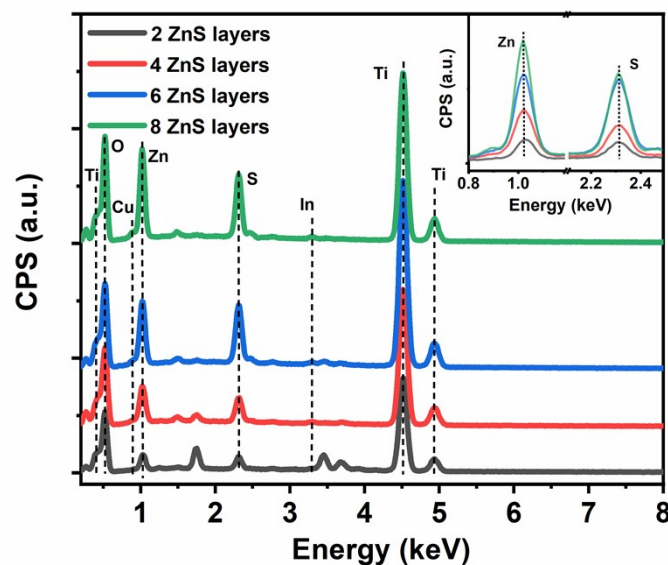


Figure S12. PEC measurements of CZIS (1Zn) QDs-sensitized photoanodes with (a) 4ZnS and (a) 8ZnS treatments under dark, continuous and chopped illumination (AM 1.5 G illumination, 100 mW/cm²).

Table S10. EDS analysis of CZIS (1Zn) QDs-based photoanodes with 2, 4, 6 and 8 ZnS monolayers.

Layers	Atom/%						Zn:Ti /%
	Ti	O	Zn	S	Cu	In	
2 ZnS	27.99	67.91	1.78	1.84	0.26	0.23	6.35
4 ZnS	28.47	63.60	4.78	2.79	0.17	0.18	16.80
6 ZnS	31.31	56.60	6.50	5.15	0.31	0.13	20.78
8 ZnS	28.10	57.69	8.14	5.39	0.48	0.19	28.95

**Figure S13.** EDS spectrum of CZIS (1Zn) QDs-based photoanodes with 2, 4, 6 and 8 ZnS monolayers. the insert is the details of Zn and S signals, which shows an obvious signal enhancement with the increasing ZnS layers.**Table S11.** PEC performance of CZIS (1Zn) QDs-based photoelectrodes with 2, 4, 6 and 8 layers ZnS in different solution.

Working electrode	Solution	J /mA·cm ⁻²	Stability
CZIS (1Zn)	A(pH~12.5)	2ZnS	56
		4ZnS	65
		6ZnS	71
		8ZnS	73
6ZnS	B(pH~7)	1.1	21

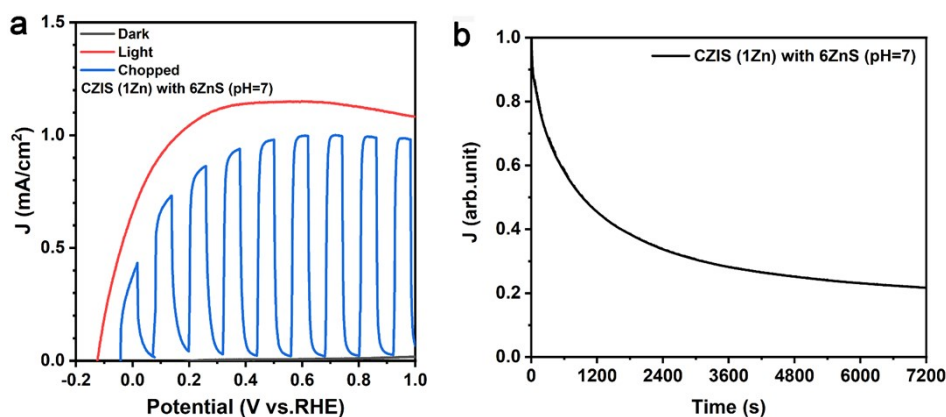


Figure S14. (a) PEC measurements of CZIS (1Zn) QDs-sensitized photoanodes with 6ZnS in electrolyte solution B (Na_2SO_4 , $\text{pH}\sim 7$) under dark, continuous, and chopped illumination (AM 1.5 G illumination, $100 \text{ mW}/\text{cm}^2$), respectively. (b) J - t curve of CZIS (1Zn) QDs-sensitized photoanode with 6 ZnS layers in electrolyte solution B ($\text{pH}\sim 7$), which were tested during 2h illumination under applied bias of 0.6 V (vs. RHE).

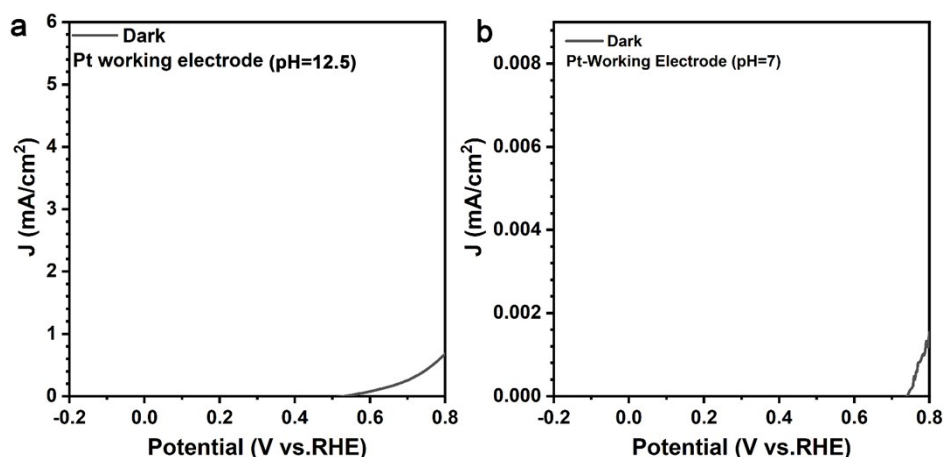


Figure S15. Electrochemistry measurements of Pt working electrode in (a) electrolyte solution A ($\text{Na}_2\text{S}/\text{Na}_2\text{SO}_3$, $\text{pH}\sim 12.5$) and (b) electrolyte solution B (Na_2SO_4 , $\text{pH}\sim 7$).

From the Figure S14 and S15, it's easy to know there is barely current in electrolyte solution A ($\text{Na}_2\text{S}/\text{Na}_2\text{SO}_3$, $\text{pH}\sim 12.5$) and electrolyte solution B (Na_2SO_4 , $\text{pH}\sim 7$) under applied bias of 0.6 V (vs RHE) if we use Pt as working electrode, which means $\text{Na}_2\text{S}/\text{Na}_2\text{SO}_3$ electrolyte provide almost electron at 0.6 V (vs. RHE) with Pt working electrode.

References

- [1] R.D. Rajapaksha, P.A. Fuierer, M.I. Ranasinghe, Sol. Energy, 189 (2019) 503-509.
- [2] C. Wang, X. Tong, W. Wang, J.-Y. Xu, L.V. Besteiro, A.I. Channa, F. Lin, J. Wu, Q. Wang, A.O. Govorov, A. Vomiero, Z.M. Wang, ACS Appl. Mater. Interfaces, 12 (2020) 36277-36286.
- [3] A.I. Channa, X. Tong, J.Y. Xu, Y.C. Liu, C.M. Wang, M.N. Sial, P. Yu, H.N. Ji, X.B. Niu, Z.M.M. Wang, J. Mater. Chem. A, 7 (2019) 10225-10230.
- [4] W. Li, L. Yao, Z. Zhang, H. Geng, C. Li, Y. Yu, P. Sheng, S. Li, Mater. Sci. Semicond. Process., 99 (2019) 106-113.

- [5] T.-L. Li, H. Teng, *J. Mater. Chem.*, 20 (2010) 3656-3664.
- [6] X. Fu, Z. Ji, C. Li, Z. Zhou, *J. Alloys Compd.*, 688 (2016) 1013-1018.
- [7] X. Tong, Y.F. Zhou, L. Jin, K. Basu, R. Adhikari, G.S. Selopal, X. Tong, H.G. Zhao, S.H. Sun, A. Vomiero, Z.M.M. Wang, F. Rosei, *Nano Energy*, 31 (2017) 441-449.
- [8] R. Wang, X. Tong, A.I. Channa, Q.G. Zeng, J.C. Sun, C. Liu, X. Li, J.Y. Xu, F. Lin, G.S. Selopal, F. Rosei, Y.N. Zhang, J. Wu, H.G. Zhao, A. Vomiero, X.P. Sun, Z.M.M. Wang, *J. Mater. Chem. A*, 8 (2020) 10736-10741.
- [9] G. Liu, Z. Ling, Y. Wang, H. Zhao, *Int. J. Hydrogen Energy*, 43 (2018) 22064-22074.
- [10] Tong, X.; Kong, X.-T.; Zhou, Y.; Navarro-Pardo, F.; Selopal, G. S.; Sun, S.; Govorov, A. O.; Zhao, H.; Wang, Z. M.; Rosei, F., *Adv. Energy Mater.* 2018, 8, 2, 1701432.